

NMR Structures of Salt-Refolded Forms of the 434-Repressor DNA-Binding Domain in 6 M Urea[†]

Konstantin Pervushin,[‡] Gerhard Wider,* Hideo Iwai,[§] and Kurt Wüthrich

Institut für Molekularbiologie und Biophysik, Eidgenössische Technische Hochschule Zürich, CH-8093 Zürich, Switzerland

Received July 15, 2004; Revised Manuscript Received September 1, 2004

ABSTRACT: The N-terminal 63-residue fragment of the phage 434-repressor, 434(1–63), has a well-defined globular fold in H₂O solution, and is unfolded in 6 M urea at pH 7.5. In this study, 434(1–63) has been refolded by adding either 1.7 M NaCl or 0.47 M NaTFA to the solution in 6 M urea, and the NMR structures of both refolded forms have been determined. The two refolded forms have similar free energies of unfolding and are ~16 kJ/mol less stable than the protein in H₂O solution. 434(1–63) refolded with NaCl exhibits NMR chemical shifts very similar to and a three-dimensional structure nearly identical to those of 434(1–63) in H₂O solution. The protein refolded with NaTFA also has a similar global fold, but it shows local differences near Phe44, of which two different orientations of the aromatic ring are compatible with the experimental data. This local conformational polymorphism attracted our interest because hydrophobic contacts between two subdomains of residues 1–36 and 45–63 are mediated by the Phe44 side chain. Anion binding experiments suggest that this polymorphism is caused by binding of TFA⁻ anions to a cluster of positively charged Arg and Lys residues located in the loop connecting the two subdomains, with apparent binding constants for TFA⁻ (K_{app}) on the order of 30 mM⁻¹.

High temperature, extreme pH values, or denaturing chemicals such as urea or guanidinium hydrochloride (GdmHCl)¹ are commonly used to investigate partially or completely unfolded states of proteins (1–4). In some cases, the unfolded proteins usually can be refolded back to a compact, collapsed state under denaturing conditions (5–8). Examples are salt-induced refolding of proteins at acidic pH (9), leading to the formation of a non-native, structured “A-state” with the characteristics of a “molten globule” (10). Multidimensional heteronuclear NMR studies of small proteins such as α -lactalbumin (11), apomyoglobin (12), barnase (13), and lysozyme (14) allowed detailed structural and dynamic characterization of salt-stabilized A-states, which typically have a high content of secondary structure, a non-native environment of the aromatic side chains, and a disordered tertiary structure when compared to the native globular fold (10, 15). It was also shown that anions can play a key role in the refolding of the A-states (16), and in

the stabilization of the native folded state from which the A-states had been derived (17). High salt concentrations that stabilize folded protein structures (17, 18) have also been shown to induce the refolding of urea- and GdmHCl-destabilized proteins (8).

The difference in the refolding of proteins from acid-unfolded states or from denaturant-unfolded states is based on an electrostatic or lyotropic stabilization mechanism, respectively (16–19). In electrostatic stabilization, anions interact specifically with positively charged groups of the protein and thus modify its internal charge distribution. Lyotropic effects depend on water–salt interactions that change the water structure, while the protein is assumed to be a passive component. It is especially intriguing to investigate salt refolding of proteins in highly concentrated denaturant solutions, since, as in the case of A-state stabilization, the anion of the salt might largely determine the physical–chemical characteristics of the refolded state (16, 18, 19).

In this paper, we report the determination of the three-dimensional structures of salt-refolded forms of the 63-residue N-terminal fragment of the phage 434-repressor, 434(1–63) (20–23), in a concentrated urea solution. The salt-refolded forms are found to be different from the molten globule state of proteins stabilized by salt at acidic pH, and specific binding of salt anions is found to destabilize local structure in the salt-stabilized global fold. Thus, the different natures of the refolding salts used here, NaCl and NaTFA, result in stabilization of two locally different refolded conformations in 6 M urea. These differences are evaluated in light of the known different electrostatic and lyotropic properties of Cl⁻ and TFA⁻ anions.

[†] Financial support was obtained from the Schweizerischer Nationalfonds (Projects 31-49047.96 and 31-66427.01).

* To whom correspondence should be addressed: Institut für Molekularbiologie und Biophysik, ETH Zürich, CH-8093 Zürich, Switzerland. Phone: +41-1-6333455. Fax: +41-1-6331073. E-mail: gsw@mol.biol.ethz.ch.

[‡] Present address: Laboratorium für Physikalische Chemie, Eidgenössische Technische Hochschule Zürich, CH-8093 Zürich, Switzerland.

[§] Present address: Department of Chemistry, University of Saskatchewan, Saskatoon, SK S7N 5C9, Canada.

¹ Abbreviations: NMR, nuclear magnetic resonance; 434(1–63), N-terminal 63-residue fragment of the phage 434-repressor; NaTFA, sodium trifluoroacetate; 2D, two-dimensional; 3D, three-dimensional; CD, circular dichroism; NOE, nuclear Overhauser effect; NOESY, NOE spectroscopy; COSY, correlation spectroscopy; DQF-COSY, double-quantum-filtered COSY; TOCSY, total correlation spectroscopy; rmsd, root-mean-square deviation; GdmHCl, guanidinium hydrochloride.

MATERIALS AND METHODS

Thermal Denaturation Measured by Circular Dichroism.

Thermal denaturation of 434(1–63) in 50 mM potassium phosphate buffer and in the presence and absence of 6 M urea and 0.04, 0.47, or 1 M NaTFA, or 1.7 M NaCl at pH 7.5, was monitored by circular dichroism at 222 nm on a Jasco J-710 spectropolarimeter with an RTE-100 thermostath using a thermostated cuvette (Omnilab) with a path length of 0.5 cm. The temperature was increased at a linear rate of 50 °C/h. The denaturation temperature (T_m), the free energy change of denaturation (ΔG_{U-N}), and the change in enthalpy at T_m (ΔH_m) were evaluated by a nonlinear fit of the CD signal intensity at 222 nm as a function of temperature. Since it is difficult to obtain precise values for the heat capacity (ΔC_p) from thermal denaturation curves, we arbitrarily decided to use a ΔC_p of 0 for the fit. For the calculations of ΔG_{U-N} , ΔC_p was approximated by assuming a value of 50 J/mol per residue multiplied by the number of residues.

Structure Determination. For the NMR measurements, uniformly ^{15}N -labeled 434-repressor(1–63) was used, which was prepared as described previously (20, 21). The sample conditions were 1 mM 434(1–63) in 50 mM potassium phosphate buffer in a 90% $\text{H}_2\text{O}/10\%$ $^2\text{H}_2\text{O}$ mixture at pH 7.5. This solution was studied in the presence and absence of 6 M urea, and with addition of variable concentrations of NaTFA between 0 and 1 M, or of NaCl between 0 and 2 M. NMR experiments were performed at 400 and 750 MHz on Varian Unity-*plus* spectrometers at 18 °C. The following NMR spectra were collected: E.COSY (24) with simultaneous presaturation of the urea and water resonances, NOESY ($\tau_m = 60$ ms) and clean-TOCSY ($\tau_m = 55$ ms) with WATERGATE water suppression (25) and presaturation of the urea resonance, 3D ^{15}N -resolved ^1H – ^1H NOESY ($\tau_m = 70$ ms), and 3D ^{15}N -resolved ^1H – ^1H TOCSY ($\tau_m = 45$ ms) (26). The NOE-based sequential assignment approach was applied to obtain sequence-specific ^1H resonance assignments (27). The strategy followed for the structure determination of 434(1–63) in 6 M urea and 0.47 M NaTFA, or in 6 M urea and 1.7 M NaCl, was essentially the same as for the previous structure determinations of 434(1–63) (23) and 434-[R10M](1–63) (21). To obtain the input for the structure calculation, proton–proton upper limit distance constraints were collected from a 3D ^{15}N -resolved ^1H – ^1H NOESY spectrum and from homonuclear 2D ^1H – ^1H NOESY spectra (27), and $^3J_{\alpha\beta}$ coupling constants were measured using E.COSY. The structure calculation was carried out with DYANA (28), and the resulting structures were energy-minimized with OPAL (29). The analysis of the structures in terms of rmsd values, atom displacements, and identification of hydrogen bonds were performed with MOLMOL (30).

The proton-to-deuterium exchange rates (k_{ex}) for 434(1–63) were measured at 18 °C by serial recordings of ^1H – ^{15}N COSY spectra started within 2 min of dissolving the lyophilized protein either in $^2\text{H}_2\text{O}$ buffered at p ^2H 4.6 (direct reading, uncorrected for isotope effects), in 6 M urea- d_4 and 0.47 M NaTFA in $^2\text{H}_2\text{O}$ at p ^2H 4.6, or in 6 M urea- d_4 and 1.7 M NaCl in $^2\text{H}_2\text{O}$ at p ^2H 4.2. In the p ^2H range of 4.2–4.6, the intrinsic exchange rates are sufficiently small to enable the detection of even relatively rapidly exchanging amide protons (27). The values of k_{rc} for the unfolded

Table 1: Thermal Denaturation of the 434(1–63) Protein Domain in Different Solvents^a

solvent	T_m^b	ΔH_m^c	ΔG_{U-N}^d
H_2O	69.0 ± 0.4	249.5 ± 3.8	24.3 ± 1.3
H_2O , 6 M urea, 1.7 M NaCl	50.8 ± 0.5	131.9 ± 3.3	7.9 ± 0.8
H_2O , 6 M urea, 0.47 M NaTFA	46.6 ± 0.5	144.4 ± 4.2	8.4 ± 0.8
H_2O , 6 M urea, 2.8 M NaCl	58.9 ± 0.5	148.6 ± 3.3	10.9 ± 0.8
H_2O , 6 M urea, 1.0 M NaTFA	56.0 ± 0.4	154.9 ± 4.2	10.5 ± 0.8

^a Thermal unfolding curves were measured in 50 mM potassium phosphate buffer at pH 7.5 by monitoring the CD signal at 222 nm. Average values and standard deviations were obtained by nonlinear fitting of the data with Kaleida-Graph (Abelbeck Software). ^b Midpoint of thermal unfolding in degrees Celsius. ^c Enthalpy change at the midpoint of thermal unfolding in kilojoules per mole. ^d Free energy change of unfolding in kilojoules per mole, calculated for 18 °C; in these calculations, a ΔC_p value of $3.2 \text{ kJ mol}^{-1} \text{ }^\circ\text{C}^{-1}$ was used, based on the assumption that ΔC_p per residue is $50 \text{ J mol}^{-1} \text{ }^\circ\text{C}^{-1}$.

proteins were estimated using acid-, base-, and water-catalyzed intrinsic exchange rates (31, 32) in the presence of high salt concentrations calculated using the web-based program SPHERE (<http://www.fccc.edu/research/labs/roder/sphere>). Since intrinsic exchange rates of model peptides are known to decrease linearly with the concentration of urea, the effect of the denaturant was taken into account using the data in Figure 2C in ref 33.

RESULTS AND DISCUSSION

Thermal Stability of the 434(1–63) Protein Domain Refolded in 6 M Urea by Addition of Salts. Refolding of 434(1–63) in 6 M urea was monitored by recording circular dichroism (CD) and ^1H – ^{15}N COSY nuclear magnetic resonance (NMR) spectra (34) at variable concentrations of NaCl or NaTFA. For both salts, plots of the CD signal at a wavelength of 222 nm versus the salt concentration in 6 M urea follow a sigmoidal curve (8), which indicates a cooperative transition of a largely unfolded protein to a refolded state (35). At NaCl and NaTFA concentrations below 200 mM, two sets of peaks were detected in the ^1H – ^{15}N COSY spectra, showing that under these conditions unfolded and refolded forms of the protein coexist with slow exchange on the chemical shift time scale. The minimal salt concentrations required for complete refolding at pH 7.5, where 434(1–63) is most stable (8), were 1.7 M NaCl or 0.47 M NaTFA, and structural studies were performed at these salt concentrations.

The change in ellipticity at 222 nm was used to calculate the free energy of denaturation (ΔG_{U-N}) and the enthalpy change (ΔH_m) at the midpoint of the denaturation at T_m (Table 1). The two forms of 434(1–63) refolded in 6 M urea with 1.7 M NaCl or 0.47 M NaTFA exhibit similar values for the melting temperature, and for the enthalpy and free energy of denaturation. Both forms are $\sim 16 \text{ kJ/mol}$ less stable than the protein in H_2O solution at pH 7.5. Amide proton-to-deuterium exchange resulted in reduced protection factors [$P = k_{\text{rc}}/k_{\text{ex}}$ (Figure 1E)], which also clearly manifests the reduced global stabilities of the refolded proteins (36); k_{rc} is the intrinsic exchange rate in the unfolded polypeptide, and k_{ex} is the measured exchange rate (37, 38).

Structure of 434(1–63) Refolded with 1.7 M NaCl in 6 M Urea. On the basis of the amide proton chemical shifts, at most minor structural changes are expected between 434(1–63) refolded with NaCl in 6 M urea and the protein in

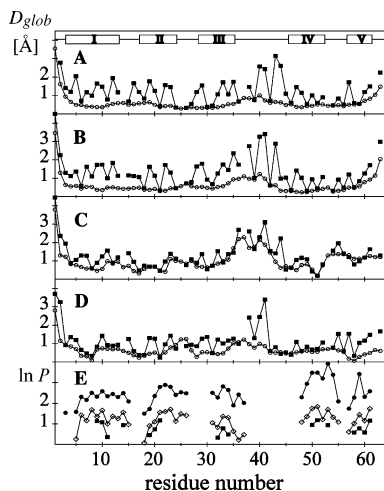


FIGURE 1: (A–D) Global displacements for backbone atoms N, C $^{\alpha}$, and C' [$D_{\text{glob}}^{\text{bb}}$ (○)] and for the side chain heavy atoms [$D_{\text{glob}}^{\text{sc}}$ (■)] plotted vs the amino acid sequence. (A and B) Average of the displacements between the 20 conformers used to represent the NMR structure and the mean structure of 434(1–63) refolded in 6 M urea with 0.47 M NaTFA and 1.7 M NaCl, respectively. (C and D) Displacements between the mean structures of 434(1–63) in H₂O solution (21) and 434(1–63) refolded in 6 M urea with 0.47 M NaTFA and 1.7 M NaCl, respectively. (E) Logarithmic plot of the protection factors, P , for exchange with solvent ^2H of the backbone amide protons of 434(1–63) in $^2\text{H}_2\text{O}$ solution (●), 434(1–63) refolded in 6 M urea in $^2\text{H}_2\text{O}$ with 0.47 M NaTFA (■), and 434(1–63) refolded in 6 M urea in $^2\text{H}_2\text{O}$ with 1.7 M NaCl (◇). Data are given for only those residues where the amide proton resonance could be observed with the real-time exchange measurements used. The locations of helices I–V are given at the top of panel A.

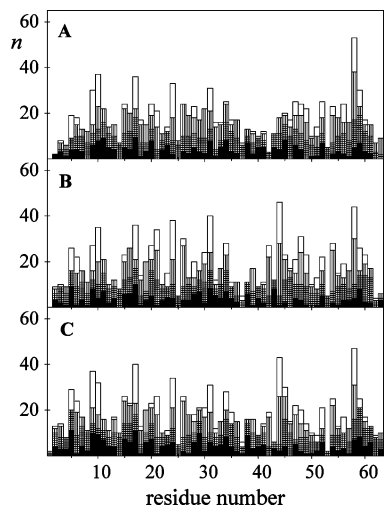


FIGURE 2: Plot of the number of NOE upper distance constraints per residue (n) vs the amino acid sequence of 434(1–63). (A) Refolded in 6 M urea with 0.47 M NaTFA. (B) Refolded in 6 M urea with 1.7 M NaCl. (C) Folded protein in H₂O solution in the absence of urea. The constraints are classified as follows: (black) intraresidual, (cross-hatched) protons in sequentially neighboring residues, (vertically hatched) protons located in residues separated by two to five positions along the sequence, and (white) longer-range constraints (27).

H₂O solution. The same conclusion comes from nearly identical distributions of NOE upper distance constraints along the sequence for 434(1–63) in H₂O, or refolded in urea with NaCl (Figure 2). This was then confirmed by the determination of the NMR structure (Figure 3 and Table 2). The global rmsd calculated for backbone atoms N, C $^{\alpha}$, and

C' between the mean structure and the 20 energy-refined conformers is 0.61 ± 0.10 Å for residues 3–60. All ϕ and ψ angles are located in the most favored and additional allowed regions of the Ramachandran plot. The data in Table 2 thus demonstrate that NMR structures of a similar high quality were obtained for the refolded and native forms of 434(1–63). The total AMBER energy for NaCl-refolded 434(1–63) is close to the AMBER energy calculated for the protein structure in H₂O solution (21). Figure 3B displays the bundle of 20 conformers that represent the conformation of 434(1–63) refolded with NaCl, which is very similar to that of the protein in H₂O solution (Figures 1D and 3A). The molecular architecture includes five α -helices comprising residues 2–13 (I), 17–24 (II), 28–35 (III), 45–52 (IV), and 56–61 (V). The data of Figure 1B,D and Table 2 confirm that the backbone fold of 434(1–63) refolded with NaCl is very similar to that of the protein in H₂O solution. The global displacements calculated for the backbone of the helical residues are smaller than 0.6 Å, and only the displacements for the loop between helices III and IV and for the chain ends are significantly larger (Figure 1D). The reduced precision reflects the near absence of long-range and medium-range NOEs in these regions (Figure 2B). It is noteworthy that 434(1–63) refolded with NaCl contains a core with tertiary packing of the amino acids similar to that of the native protein (Figure 3A,B). Often when unfolded proteins are refolded from usually denaturing conditions to a collapsed state, they form molten globules with a disordered tertiary structure when compared to the native globular fold (10–15).

Structure of 434(1–63) Refolded with 0.47 M NaTFA in 6 M Urea. In contrast to the 434(1–63) refolded in 6 M urea with NaCl, the protein refolded with NaTFA showed some significant local deviations of proton chemical shifts from those of the protein in H₂O solution, in particular for H^N of Arg43, Phe44, and Ile45, with differences of 0.28, 1.61, and 0.48 ppm, respectively. The largest difference observed for an aliphatic proton is 0.98 ppm for H ^{β} of Pro42. Conversely, the NOESY cross-peak network is similar to the one of the protein in H₂O solution, except for the long-range NOEs with aromatic ring protons of Phe44, which showed an \sim 5-fold reduction in intensity when compared to the corresponding NOEs found for 434(1–63) in aqueous solution, and the appearance of additional weak NOEs between the aromatic protons of Phe44 and the backbone protons of Arg43. Structure calculations with DYANA (28) resulted in a high-quality globular NMR structure, as evidenced by a low global rmsd and good Ramachandran statistics (Table 2) as well as by similar tertiary packing of the refolded and the native forms of 434(1–63) (Figure 3A,C). This structure is very similar to the structure of 434(1–63) in H₂O solution (Figure 1C and Table 2). A set of 24 NOE constraints was identified, which all were consistently violated in the calculated structures and which all involve the side chain of Phe44. When the calculations were repeated without these constraints, a bundle of 20 protein conformers containing two alternative positions of the aromatic ring of Phe44 was obtained (Figure 4). In 12 of the 20 conformers, the position of the aromatic ring corresponds closely to that of 434(1–63) in H₂O solution, where it is in a hydrophobic pocket formed by the side chains of Val24, Ile31, Leu34, Pro42, and Leu48. In the remaining

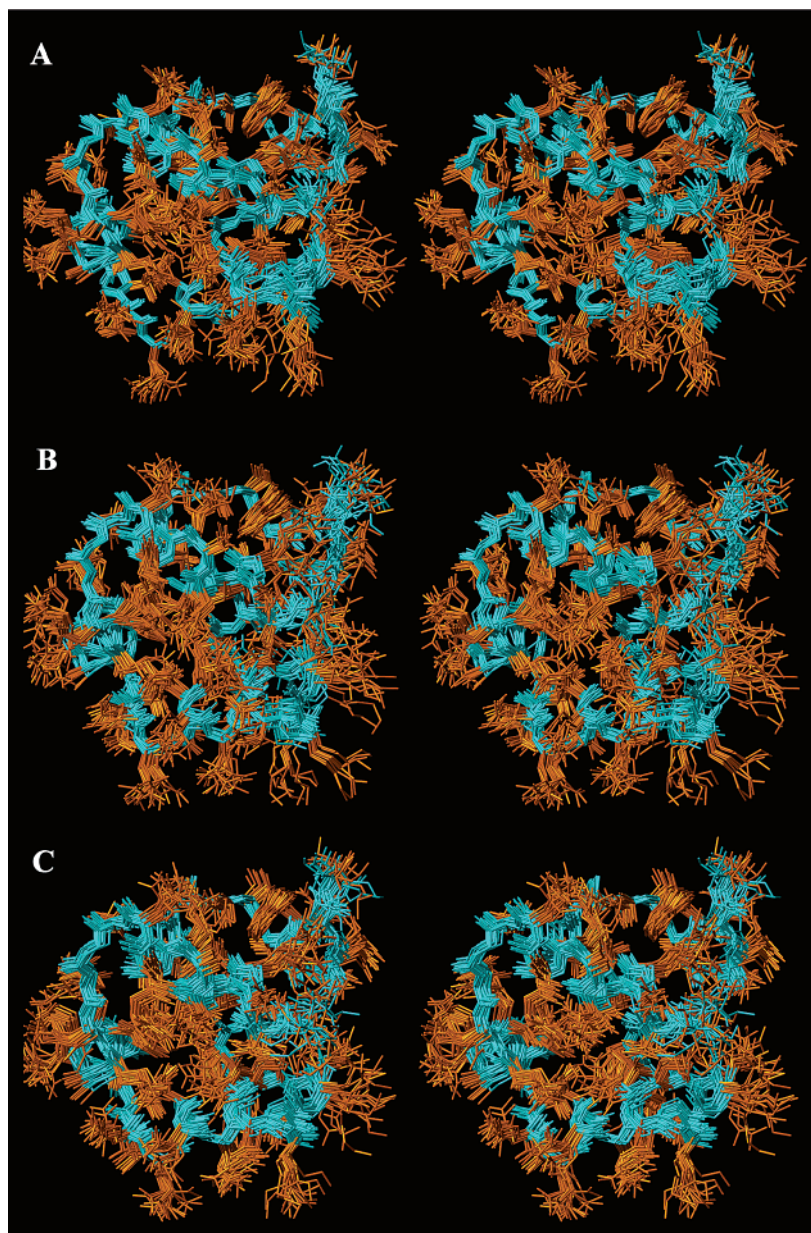


FIGURE 3: Stereoviews of all-heavy-atom representations of bundles of 20 energy-minimized DYANA conformers of 434(1–63): (A) in H₂O solution at 18 °C and pH 7.5, (B) refolded in 6 M urea with 1.7 M NaCl at 18 °C and pH 7.5, and (C) refolded in 6 M urea with 0.47 M NaTFA at 18 °C and pH 7.5. Backbone atoms N, C^α, and C' of residues 3–60 were superimposed for a minimal rmsd. The backbone is colored blue, and the side chains are colored brown.

eight conformers, the Phe44 side chain is rotated out of this pocket toward the protein surface. For the two subgroups of 434(1–63) structures (Figure 4), ring current shift calculations (Figure 5A) reproduced the experimental proton chemical shift differences (Figure 5B) remarkably well. Since only a single set of proton resonances was found in the experimental spectra, we conclude that the rate of exchange between the two orientations of the Phe44 side chain is significantly faster than the chemical shift differences between the two conformations, i.e., faster than 1000 s⁻¹.

Binding of TFA⁻ Anions to 434(1–63) in H₂O Solution and to 434(1–63) Refolded in 6 M Urea. Specific binding of salts to 434(1–63) was monitored by collecting a series of ¹H–¹⁵N COSY spectra in H₂O solution at pH 7.5 after addition of variable concentrations of NaCl or NaTFA. A titration of the protein solution with NaCl showed no significant change in ¹H and ¹⁵N chemical shifts. In contrast,

a titration with NaTFA caused sizable changes in the ¹H and ¹⁵N resonance positions of Arg43, Phe44, and Ile45 (Figure 6 A), and also of ¹⁵N of Gly25 and Thr39, while most of the other residues were hardly affected. The chemical shifts can be attributed to specific anion binding, since the two salts share the Na⁺ cation but only NaTFA causes significant chemical shifts. Considering the pronounced selectivity of the effect of TFA⁻ binding to only five residues, it is to be attributed to a localized change of the protein structure near specific anion-binding sites, rather than to a perturbation of the global structure.

The chemical shift dependence of some amide moieties on the NaTFA concentration has been used to quantitate the binding process. If binding of *N* mol of the anion (X) to 1 mol of protein with intrinsic binding constants (*K_i*) shifts the conformational equilibrium between the free protein (A) and liganded forms (AX, AX₂, ..., AX_{*N*}), then the observable

Table 2: Analysis of the Bundles of 20 Energy-Minimized DYANA Conformers of 434(1–63) in 6 M Urea Refolded either with 0.47 M NaTFA or with 1.7 M NaCl, and Comparison with the Structure of 434(1–63) in H₂O Solution

	refolded with 0.47 M NaTFA	refolded with 1.7 M NaCl
no. of input constraints		
upper distance limits from NOEs	661	696
ϕ , ψ , and χ^1 torsion angle constraints ^a	145	148
stereospecific assignments	36	38
DYANA residual target function value (Å ²) ^b	0.11 ± 0.1	0.43 ± 0.15
NOE violations >0.1 Å	0.6 ± 0.12	1.8 ± 0.24
torsion angle violations >2.5°	0.0 ± 0.0	0.1 ± 0.04
total AMBER energy (kJ/mol)	−8540 ± 200	−8500 ± 230
rmsd (Å)		
bb (3–60) ^{c,d}	0.57 ± 0.10	0.61 ± 0.10
all heavy atoms (3–60) ^d	1.16 ± 0.10	1.24 ± 0.16
bb (3–60) H ₂ O/refolded ^e	1.07	0.66
bb (3–35) ^{c,d}	0.46 ± 0.08	0.49 ± 0.11
all heavy atoms (3–35) ^d	1.01 ± 0.11	1.09 ± 0.16
bb (3–35) H ₂ O/refolded ^e	0.65	0.49
bb (46–60) ^{c,d}	0.27 ± 0.06	0.27 ± 0.07
all heavy atoms (46–60) ^d	0.65 ± 0.06	0.61 ± 0.07
bb (46–60) H ₂ O/refolded ^e	0.34	0.29
Ramachandran statistics (%) ^f		
residues in the most favored regions	84	81
residues in additional allowed regions	16	19
residues in generously allowed regions	0	0
residues in the disallowed regions	0	0

^a These constraints include the information obtained from the measurement of coupling constants: 53 ³J_{HN α and 34 ³J _{$\alpha\beta$ coupling constants were determined for 434(1–63) refolded with 0.47 M NaTFA, and the corresponding numbers for 434(1–63) refolded with 1.7 M NaCl are 53 and 37, respectively. ^b Before energy minimization. ^c bb stands for backbone heavy atoms N, C α , and C'. The numbers in parentheses indicate the residues which were used for minimal rmsd superposition. ^d The global rmsd is given as the average of the pairwise rmsd values between each of the 20 energy-refined DYANA (28) conformers and the mean structure. ^e The rmsd between the mean structures of 434(1–63) in H₂O (21) and in the refolded form. ^f The Ramachandran statistics was calculated with DYANA (28).}}

equilibrium constant K_{app} can be written as

$$K_{app} = ([AX] + [AX_2] + \dots)/A_{tot} = 1/(1 + [X]K_1 + [X]^2K_2 + \dots) \quad (1)$$

For noncompetitive binding, the average number of anions bound per protein molecule (\bar{N}) can be calculated as

$$\bar{N} = d(\ln K_{app})/d(\ln[X]) \quad (2)$$

Values for K_{app} were calculated from the equation $K_{app} = (Y - Y_0)/(Y_1 - Y)$, where Y is the observed chemical shift of a particular amide proton and Y_0 and Y_1 are the corresponding values for the free and bound states, respectively, based on the chemical shifts of the NaTFA-free and fully NaTFA-saturated form of the protein (Figure 6A). Figure 6B shows plots of $\ln K_{app}$ versus the logarithm of the anion concentration for the three residues of Figure 6A, which resulted in values for \bar{N} of 1.09, 1.10, and 0.87 for Arg43, Phe44, and Ile45, respectively.

The intrinsic binding constant for the titratable residues (K_b) was evaluated by fitting the data in Figure 6A to a simple two-state binding equation (35):

$$K_{app} = 1/(1 + [X]K_b) \quad (3)$$

The inverse value of the binding constant corresponds to the anion concentrations of the transition midpoint, which are 30.1 ± 0.5 , 31.9 ± 0.6 , and 37.0 ± 0.9 mM for Arg43, Phe44, and Ile45, respectively. The result indicates that only one TFA[−] anion binds to each binding site on the protein surface, and that there is no cooperative interaction between multiple anions bound. The analysis of eqs 1–3 cannot give the total number of binding sites. Nonetheless, the fact that similar values of $1/K_{app}$ were obtained for Arg43 and Phe44, whereas $1/K_{app}$ of Ile45 is slightly different, may suggest that in addition to the binding site situated close to residues Arg43 and Phe44, an additional, lower-affinity TFA[−] binding site might be present in the vicinity of Phe44.

Structure-Stabilizing Mechanisms. Three factors might contribute to the refolding of 434(1–63) by 1.7 M NaCl or 0.47 M NaTFA in the presence of 6 M urea at neutral pH, where this protein is otherwise unfolded. These are the Debye–Hückel electrostatic screening effect of ions, the lyotropic effect of anions on the water structure, and anion binding to the protein (16). The experimental result that the refolding transitions induced by NaCl or NaTFA are dependent on the anion would be inconsistent with the Debye–Hückel electrostatic screening effect being a major factor. To allow comparison of the effects of NaCl and NaTFA at identical ionic strengths, we added 1.23 M NaBr to the protein solution in 6 M urea and 0.47 M NaTFA, whereby NaBr was selected for its weak lyotropic efficacy (39). The addition of 1.23 M NaBr caused no significant changes in the ¹H or ¹⁵N chemical shifts of the refolded protein, indicating that there is at most a negligibly small dependence of the protein refolding on the overall ionic strength of the solution.

All data that were obtained are consistent with the lyotropic effect being the major stabilization factor of the salt additives on the 434(1–63) structure in 6 M urea. The refolding efficacy of anions follows the Hofmeister series of anions; i.e., TFA[−] has a stronger effect on the water structure than Cl[−] (19, 39), and consequently, less TFA[−] is required to bring about refolding of 434(1–63) in 6 M urea. Denaturation studies at variable salt concentrations (Table 1) showed that the transition temperature and the free energy of denaturation of the refolded protein increase monotonically with the amount of salt used, which would also be consistent with lyotropic stabilization (39). Further, it was observed that refolding of 434(1–63) in 6 M urea can also be achieved with molar concentrations of nonionizable compounds, for example, glucose (8), which can also cause lyotropic stabilization (18).

Binding of an anion to positively charged groups in the protein has been identified as the major factor responsible for anion-induced refolding from acid-denatured states to the compact, non-native A-state (16). Since the stabilization effect is determined by the particular distribution of charges and the affinity of the anions for each of the potential binding sites, refolding strongly depends on the anion species and is usually incomplete, leading to the formation of non-native, molten globule states (15, 16). To investigate possible effects of specific TFA binding in the system being studied here, the interactions of TFA[−] with folded 434(1–63) in aqueous solution were monitored in a series of NMR spectra. Stabilization of a non-native conformation of the polypeptide at concentrations of 2–30 mM NaTFA was found, and a

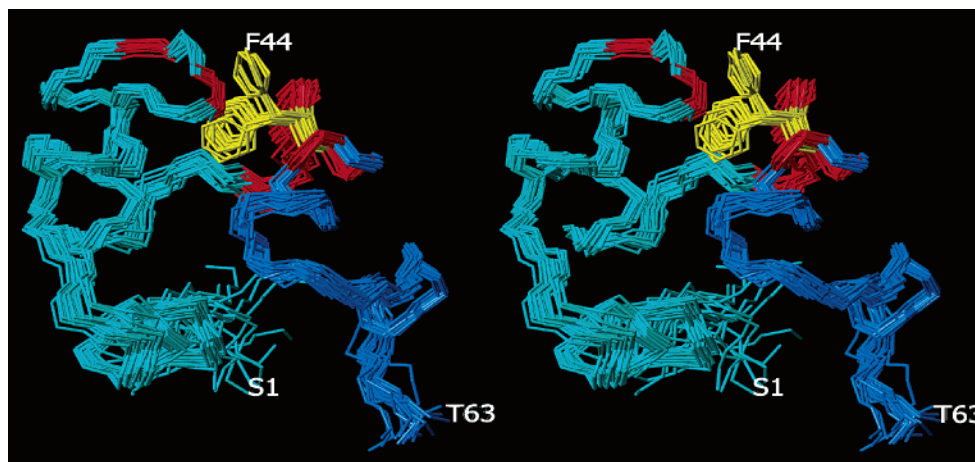


FIGURE 4: Stereoview of a bundle of 20 energy-minimized DYANA conformers of 434(1–63) refolded in 6 M urea with 0.47 M NaTFA. Backbone atoms N, C α , and C' of residues 3–60 were superimposed for a minimal rmsd. Subdomains I (residues 2–35) and II (residues 45–60) are colored cyan and blue, respectively. All heavy atoms are shown for Phe44 (yellow), which shows two sub-bundles of locally different conformers. Residues colored red contain at least one proton with a chemical shift difference of >0.15 ppm when compared to the corresponding proton in 434(1–63) in H₂O solution.

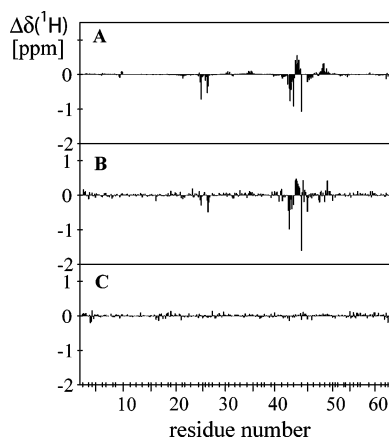


FIGURE 5: Plots of the proton chemical shift differences [$\Delta\delta(^1\text{H})$] between different folded forms of the protein vs the sequence of 434(1–63). The intervals between successive vertical ticks on the abscissa are proportional to the number of assigned protons of the particular residue. The amplitudes of the vertical bars represent the sums of the chemical shift differences of all protons in the residue. (A) Chemical shift differences predicted from ring current calculations using MOLMOL (30) between the two conformers of 434(1–63) refolded with NaTFA in urea, one with the same position of the aromatic ring of Phe44 that is seen in the folded protein in H₂O solution and one with the solvent-exposed position of the Phe44 side chain (Figure 4). (B) Experimental chemical shift differences between 434(1–63) in 6 M urea refolded with NaTFA and 434(1–63) in H₂O solution. (C) Experimental chemical shift differences between 434(1–63) refolded with NaCl in 6 M urea and 434(1–63) in H₂O solution. In panels B and C, the protein in H₂O was assessed at pH 4.8, and the refolded proteins were assessed at pH 7.5.

TFA[−] concentration of 30 mM is sufficient for occupation of half of the anion binding sites of 434(1–63) in H₂O solution (Figure 6A). For refolding of 434(1–63) in 6 M urea, a significantly higher concentration of TFA[−] is required, with 0.16 M TFA[−] refolding half of the 434(1–63) molecules. This observation suggests that binding of TFA[−] to the protein is unlikely to be the major factor in refolding. Rather, it is responsible for a local modification of the protein structure, independent of the additional presence of urea. Thus, our data indicate for both salts that the major contribution to refolding is the Hofmeister stabilization. The

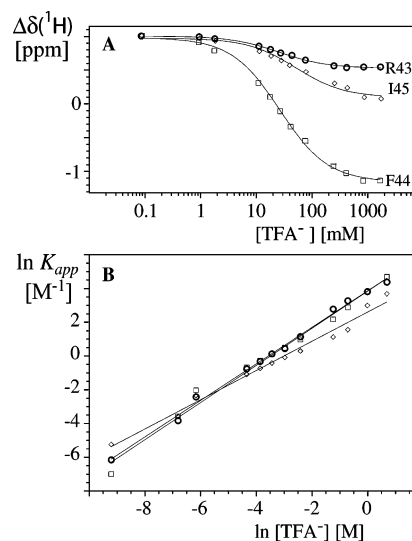


FIGURE 6: (A) Chemical shift deviations relative to the protein in H₂O solution (23) [$\Delta\delta(^1\text{H})$] of amide protons of 434(1–63) at pH 7.5 in an aqueous NaTFA solution vs the NaTFA concentration. Data are shown for Arg43, Phe44, and Ile45, which are unique in that a strong dependence on the NaTFA concentration was found (see the text). The lines through the experimental points represent fits of the data with eq 3. (B) Plot of $\ln K_{app}$ vs $\ln[\text{NaTFA}]$, representing binding of TFA[−] to 434(1–63) according to eq 2. The same symbols as in panel A are used to represent R43, F44, and I45.

molecular mechanism of the Hofmeister effect is not sufficiently well-known to explain why a significantly lower concentration of TFA[−] than of Cl[−] anions is required for refolding.

In conclusion, the structure of 434(1–63) in 6 M urea refolded with NaCl coincides nearly identically with that of 434(1–63) in H₂O solution, albeit with a somewhat reduced stability for the refolded form. In contrast, the structural and dynamic features of 434(1–63) in 6 M urea refolded with 0.47 M NaTFA indicate that under these conditions the protein adopts a folded state which is reminiscent of a “highly ordered molten globule” (11). This is supported by further reduced values of the amide proton exchange protection factors, when compared to those in the NaCl-refolded form

(Figure 1E), and by the observation that the time-averaged structure is close to but not identical with the one in H₂O solution.

REFERENCES

- Deyoung, L. R., Dill, K. A., and Fink, A. L. (1993) Aggregation and denaturation of apomyoglobin in aqueous urea solutions, *Biochemistry* 32, 3877–3886.
- Alonso, D. O. V., Dill, K. A., and Stigter, D. (1991) The 3 states of globular proteins: acid denaturation, *Biopolymers* 31, 1631–1649.
- Alonso, D. O. V., and Dill, K. A. (1991) Solvent denaturation and stabilization of globular proteins, *Biochemistry* 30, 5974–5985.
- Neri, D., Billeter, M., Wider, G., and Wüthrich, K. (1992) NMR determination of residual structure in a urea-denatured protein, the 434-repressor, *Science* 257, 1559–1563.
- Nishimura, C., Uversky, V. N., and Fink, A. L. (2001) Effect of salts on the stability and folding of staphylococcal nuclease, *Biochemistry* 40, 2113–2128.
- Uversky, V. N., Karnoup, A. S., Segel, D. J., Seshadri, S., Doniach, S., and Fink, A. L. (1998) Anion-induced folding of staphylococcal nuclease: characterization of multiple equilibrium partially folded intermediates, *J. Mol. Biol.* 278, 879–894.
- Goto, Y., and Fink, A. L. (1994) Acid-Induced Folding of Heme-Proteins, *Hemoglobins* (Part C), 3–15.
- Dötsch, V., Wider, G., Siegal, G., and Wüthrich, K. (1995) Salt-stabilized globular protein structure in 7 M aqueous urea solution, *FEBS Lett.* 372, 288–290.
- Fink, A. L., Calciano, L. J., Goto, Y., Kurotsu, T., and Palleros, D. R. (1994) Classification of acid denaturation of proteins: intermediates and unfolded states, *Biochemistry* 33, 12504–12511.
- Ptitsyn, O. B. (1995) Molten globule and protein folding, *Adv. Protein Chem.* 47, 83–229.
- Redfield, C., Schulman, B. A., Milhollen, M. A., Kim, P. S., and Dobson, C. M. (1999) α -Lactalbumin forms a compact molten globule in the absence of disulfide bonds, *Nat. Struct. Biol.* 6, 948–952.
- Loh, S. N., Kay, M. S., and Baldwin, R. L. (1995) Structure and stability of a 2nd molten globule intermediate in the apomyoglobin folding pathway, *Proc. Natl. Acad. Sci. U.S.A.* 92, 5446–5450.
- Arcus, V. L., Vuilleumier, S., Freund, S. M. V., Bycroft, M., and Fersht, A. R. (1995) A Comparison of the pH-, urea- and temperature-denatured states of barnase by heteronuclear NMR-implications for the initiation of protein folding, *J. Mol. Biol.* 254, 305–321.
- Morozova, L. A., Haynie, D. T., Aricomuendel, C., Vandael, H., and Dobson, C. M. (1995) Structural basis of the stability of a lysozyme molten globule, *Nat. Struct. Biol.* 2, 871–875.
- Ptitsyn, O. B. (1995) How the molten globule became, *Trends Biochem. Sci.* 20, 376–379.
- Goto, Y., Takahashi, N., and Fink, A. L. (1990) Mechanism of acid-induced folding of proteins, *Biochemistry* 29, 3480–3488.
- Ramos, C. H. I., and Baldwin, R. L. (2002) Sulfate anion stabilization of native ribonuclease A both by anion binding and by the Hofmeister effect, *Protein Sci.* 11, 1771–1778.
- Timasheff, S. N., and Arakawa, T. (1990) Stabilization of protein structure by solvents, in *Protein Structure, a Practical Approach* (Creighton, T. E., Ed.) pp 331–335, Oxford University Press, Oxford, U.K.
- Collins, K. D., and Washabaugh, M. W. (1985) The Hofmeister effect and the behaviour of water at interfaces, *Q. Rev. Biophys.* 18, 323–422.
- Neri, D., Wider, G., and Wüthrich, K. (1992) H-1, N-15 and C-13 NMR assignments of the 434 repressor fragments 1–63 and 44–63 unfolded in 7 M urea, *FEBS Lett.* 303, 129–135.
- Pervushin, K., Billeter, M., Siegal, G., and Wüthrich, K. (1996) Structural role of a buried salt bridge in the 434 repressor DNA-binding domain, *J. Mol. Biol.* 264, 1002–1012.
- Mondragon, A., Subbiah, S., Almo, S. C., Drottler, M., and Harrison, S. C. (1989) Structure of the amino-terminal domain of phage 434 repressor at 2.0 Å resolution, *J. Mol. Biol.* 205, 1989–2001.
- Neri, D., Billeter, M., and Wüthrich, K. (1992) Determination of the nuclear magnetic resonance solution structure of the DNA-binding domain (residues 1 to 69) of the 434-repressor and comparison with the X-ray crystal structure, *J. Mol. Biol.* 223, 743–767.
- Griesinger, C., Sørensen, O. W., and Ernst, R. R. (1987) Practical aspects of the E.COSY technique: measurement of scalar spin-spin coupling constants in peptides, *J. Magn. Reson.* 75, 474–492.
- Piotto, M., Saudek, V., and Sklenar, V. (1992) Gradient-tailored excitation for single-quantum NMR spectroscopy of aqueous solutions, *J. Biomol. NMR* 2, 661–665.
- Cavanagh, J., Fairbrother, W. J., Palmer, A. G., and Skelton, N. J. (1996) *Protein NMR Spectroscopy: Principles and Practice*, Academic Press, New York.
- Wüthrich, K. (1986) *NMR of Proteins and Nucleic Acids*, Wiley, New York.
- Güntert, P., Mumenthaler, C., and Wüthrich, K. (1997) Torsion angle dynamics for NMR structure calculation with the new program DYANA, *J. Mol. Biol.* 273, 283–298.
- Luginbühl, P., Güntert, P., Billeter, M., and Wüthrich, K. (1997) The new program OPAL for molecular dynamics simulations and energy refinements of biological macromolecules, *J. Biomol. NMR* 9, 212–212.
- Koradi, R., Billeter, M., and Wüthrich, K. (1996) MOLMOL: a program for display and analysis of macromolecular structures, *J. Mol. Graphics* 14, 51–55.
- Bai, Y. W., Sosnick, T. R., Mayne, L., and Englander, S. W. (1995) Protein folding intermediates: native-state hydrogen exchange, *Science* 269, 192–197.
- Chamberlain, A. K., and Marqusee, S. (1998) Molten globule unfolding monitored by hydrogen exchange in urea, *Biochemistry* 37, 1736–1742.
- Loftus, D., Gbenle, G. O., Kim, P. S., and Baldwin, R. L. (1986) Effects of denaturants on amide proton exchange rates: a test for structure in protein fragments and folding intermediates, *Biochemistry* 25, 1428–1436.
- Wider, G. (1998) Technical aspects of NMR spectroscopy with biological macromolecules and studies of hydration in solution, *Prog. Nucl. Magn. Reson. Spectrosc.* 32, 193–275.
- Poland, D. (1978) *Cooperative Equilibria in Physical Biochemistry*, pp 1–55, Clarendon Press, Oxford, U.K.
- Wagner, G., and Wüthrich, K. (1978) Dynamic model of globular protein conformations based on NMR studies in solution, *Nature* 275, 247–248.
- Englander, S. W., Sosnick, T. R., Englander, J. J., and Mayne, L. (1996) Mechanisms and uses of hydrogen exchange, *Curr. Opin. Struct. Biol.* 6, 18–23.
- Christoffersen, M., Bolvig, S., and Tuchsén, E. (1996) Salt effects on the amide hydrogen exchange of bovine pancreatic trypsin inhibitor, *Biochemistry* 35, 2309–2315.
- Cacace, M. G., Landau, E. M., and Ramsden, J. J. (1997) The Hofmeister series: salt and solvent effects on interfacial phenomena, *Q. Rev. Biophys.* 30, 241–277.

BI048496A